Polymer/Clay Nanocomposites Through Multiple Hydrogen-bonding Interactions

Muhammed Aydin,[1] Tamer Uyar,[2] Mehmet Atilla Tasdelen,[3] Yusuf Yagci[1,4]

[1]Department of Chemistry, Istanbul Technical University, 34469, Maslak, Istanbul, Turkey
[2]UNAM-Institute of Materials Science and Nanotechnology, Bilkent University, 06800 Ankara, Turkey
[3]Department of Polymer Engineering, Faculty of Engineering, Yalova University, 77100 Yalova, Turkey
[4]Center of Excellence for Advanced Materials Research (CEAMR) and Department of Chemistry, Faculty of Science, King Abdulaziz University, 21589, Jeddah, Saudi Arabia
Correspondence to: Y. Yagci (E-mail: yusuf@itu.edu.tr) or M. A. Tasdelen (E-mail: tasdelen@yalova.edu.tr)

ABSTRACT: An 2-ureido-4[1H]pyrimidinone (UPy) motif with self-association capability (through quadruple hydrogen bonds) was successfully anchored onto montmorillonite clay layers. Polymer/clay nanocomposites were prepared by specific hydrogen bonding interactions between surface functionalized silica nanoclays and UPy-bonded supramolecular poly(ethylene glycol) or poly(ε-caprolactone). The mixed morphologies including intercalated layers with a non-uniform separation and exfoliated single layers isolated from any stack were determined by combined X-ray diffraction and transmission electron microscopic measurements. Thermal analyses showed that all nanocomposites had higher decomposition temperatures and thermal stabilities compared with neat polymer. The differential scanning calorimetric data implied that the crystallinity of polymers did not show essential changes upon introduction of organomodified UPy clays. © 2014 Wiley Periodicals, Inc. J. Polym. Sci., Part A: Polym. Chem. **2015**, *53*, 650–658

KEYWORDS: hydrogen bonding; nanocomposites; organoclay; ring-opening polymerization; self-assembly

INTRODUCTION Over the last two decades, various types of nanofillers have been used for the preparation of nanocomposites with almost all types of polymer matrices.[1] However, polymer nanocomposites based on clays attract great interest in today's materials research because they are naturally abundant, economical, and more important, benign to the environment.[2] But the dispersion of this kind of nanofillers is not straightforward. In most cases, surface modification of these materials is required to obtain organically modified silicates or clay which then is more compatible with the organic polymer matrices. Generally, the addition of small amount of clay into polymer-based materials resulted in an impressive property enhancements, such as high moduli, increased strength and heat resistance, decreased gas permeability, and flammability.[3]

Up to date, a number of synthesis routes have been developed to fabricate polymer nanocomposites with homogenous dispersion of clay layers, in solution mixing, melt mixing, and *in-situ* polymerization.[4] Due to the direct synthesis via polymerization along with the presence of organoclays, the *in-situ* polymerization is most widely used technique to produce polymer nanocomposites with homogeneous distribution of the clay layers inside the polymer matrix.[5,6] In this route, organoclay containing monomer, initiator, or catalyst functionalities is first dispersed in the monomer or monomer solution, and then the resulting mixture is polymerized by standard polymerization methods. The *in-situ* polymerization can be initiated by external stimulation such as thermal,[7–10] photochemical,[11–20] or chemical activation. The growth of polymer chains within the clay galleries may lead to the clay exfoliation and hence the nanocomposite formation.[21–24] Recently, a conceptually different approach, namely copper (I) catalyzed azide/alkyne cycloaddition (CuAAC) "click" reaction, in which exfoliation is rooted in the functional units of the intercalant that readily react with the antagonist groups of the preformed polymers.[25–28] In this approach, azide and alkyne partners could each be incorporated in either the clay surface or polymer chain. The quantitative efficiency of coupling reaction coupled with tolerance to a wide variety of functional groups and reaction conditions make this coupling process highly attractive for the nanocomposite preparation.

Molecular self-assembly is a powerful method for the construction of well-defined nanoarchitectures and for the

Additional Supporting Information may be found in the online version of this article.

tailoring of physical properties of small molecular building blocks.[29,30] With this method, a variety of nanostructures including micelles, vesicles, liquid crystal phases, and Langmuir monolayers by surfactant molecules and supramolecular assemblies can be constructed by means of non-covalent interactions, such as hydrogen bonding, metal coordination, hydrophobic forces, van der Waals forces, π–π stacking, and/or electrostatic interactions. Among them, hydrogen bonding system is the most crucial and favorite secondary interaction to construct supramolecular architectures due to their moderate strength, high directionality, and selectivity. However, the hydrogen bond pairs are weak relative to covalent and ionic bonds, and therefore, the application of synthetic hydrogen bonding systems require the use of multiple hydrogen-bonding interactions. In this regard, 2-ureido-4[1H]pyrimidinone (UPy) functionality is a promising unit which can undergo very strong and highly directional self-complimentary quadruple hydrogen bonding through their dimerization.[31] The UPy-based hydrogen-bonding system has been applied for the preparation of supramolecular polymers[32,33] from the corresponding telechelics prepared with a variety of polymer backbones including poly(ethylene oxide)s,[34] poly(butadiene)s,[35] poly(dimethyl siloxane)s,[36] poly(styrene)s,[37] and poly(methyl methacrylate)s.[37,38] However, this chemistry has been scarcely applied for the preparation of supramolecular polymer nanocomposites using graphenes, carbon nanotubes, and gold hydroxyapatite and silica nanoparticles as nanofiller. To the best of our knowledge, no report is currently available in open literature regarding the use of UPy-based hydrogen-bonding system in the preparation of polymer/clay nanocomposites.

In the present study, we synthesized an UPy-functionalized organoclay from commercial montmorillonite (MMT) clay (Closite 30B) containing two hydroxyl groups by urethane formation with UPy-isocyanate. The UPy-end functionalized poly(ethylene glycol) and poly(ε-caprolactone) (PCL) were chosen as matrix polymer for nanocomposites due to their synthetic accessibilities and existing knowledge on their characterizations. The multiple hydrogen-bonding interactions of the intercalated UPy-functionalized organoclay and UPy-end functionalized polymers could gradually push the layers apart, leading to delamination of clay tactoids and leading to formation of nanocomposites. The synthetic capabilities of this approach can be greatly extended by careful choices of organoclays and polymers, and the optimization of supramolecular interactions as well.

EXPERIMENTAL

Materials

Organo-modified clay, Cloisite 30B [MMT-$(CH_2CH_2OH)_2$] was purchased from Southern Clay Products (Gonzales, TX). The organic content of the organo-modified MMT, determined by thermogravimetric analysis (TGA), was 21 wt %. Before use, the clay was dried under vacuum at 110 °C for 1 h. Tin(II) 2-ethyl-hexanoate [Sn(Oct)$_2$, Aldrich, 95%], poly(ethylene glycol) methyl ether (Me-PEG, Aldrich, $M_w = 2000$ g/mol),

2-amino-4-hydroxy-6-methylpyrimidine (Aldrich, 98%), hexamethylene diisocyanate (HMDI, Aldrich, ≤99%), dibutyltin dilaurate (Aldrich, 95%), 1-butanol (Merck, 99.5%), pyridine (Merck, 98%), ethanol (Merck, 96%), pentane (Merck, 98%), acetone (Merck, ACS), toluene (Merck, 99%), and hydrochloric acid (HCl, Merck, 32%) were used as received. Epsilon-caprolactone (CL, Aldrich, 97%) was vacuum distilled over calcium hydride.

Synthesis of 2-(6-Isocyanatohexylamino carbonylamino)-6-methyl 4[1H] pyrimidinone (UPy-Isocyanate)

UPy-isocyanate was prepared according to the modified literature procedure.[39] 2-Amino-4-hydroxy-6-methyl pyrimidine (8.6 g, 70 mmol) was added to a 250 mL round bottomed flask. 1,6-Hexamethylene diisocyanate (HMDI, 76 mL, 475 mmol) and pyridine (5 mL) were then added, the flask was fitted with a reflux condenser, and the mixture was stirred at 100 °C overnight under dry nitrogen. Pentane (30 mL) was then added and the solid product, a white powder, was collected by filtration. The solid product was washed three times with 125 mL portions of acetone to remove unreacted HMDI and then was dried overnight under high vacuum at 50 °C (18.5 g; yield: 90%).

^{1}H-NMR (CDCl$_3$): δ = 13.14 (s, 1H, CH$_3$—C—N<u>H</u>), 11.87 (s, 1H, CH$_2$—NH—(C=O)—N<u>H</u>), 10.19 (t, 1H, CH$_2$—N<u>H</u>—(C=O)—NH), 5.82 (s, 1H, C<u>H</u>=C—CH$_3$), 3.27 (m, 4H, NH—(C=O)—NH—C<u>H</u>$_2$ + C<u>H</u>$_2$—NCO), 2.23 (s, 3H, C<u>H</u>$_3$), 1.61 (m, 4H, N—CH$_2$—C<u>H</u>$_2$), 1.41 (m, 4H, CH$_2$—CH$_2$—C<u>H</u>$_2$—C<u>H</u>$_2$—CH$_2$—CH$_2$—NCO) ppm.

FT-IR (ATR): υ = 3320, 2930, 2260 (NCO stretch), 1700 (UPy), 1670 (UPy), 1620 (urea), 1580 (UPy), 1520 (UPy), 1460, 1355, 1310, 1255 cm^{-1}.

Synthesis of UPy-End Functionalized Poly(ethylene glycol) (PEG-UPy)

Me-PEG (2000 mg, 1 mmol) was first dried under vacuum at 90 °C and then dissolved in dry CHCl$_3$. The UPy-isocyanate (880 mg, 3 mmol) and three drops of dibutyltin dilaurate (DBDTL) were added to the reaction mixture, which was stirred at 60 °C for 16 h. The crude product was precipitated in cold methanol, filtered, and dried under vacuum (1.3 g; yield: 65%).

^{1}H-NMR (CDCl$_3$): δ = 13.12 (s, 1H, C—N<u>H</u>—C=N, UPy), 11.84 (s, 1H, CH$_2$NH—(C=O)—N<u>H</u>, UPy), 10.11 (s, 1H, CH$_2$N<u>H</u>—(C=O)—NH, UPy), 5.83 (s, 1H, C=C<u>H</u>, UPy), 4.92 (s, 1H, CH$_2$N<u>H</u>—(C=O)—OCH$_2$), 4.18 (t, 2H, NH—(C=O)—OC<u>H</u>$_2$CH$_2$), 3.74 (t, 2H, NH—(C=O)—OCH$_2$C<u>H</u>$_2$), 3.64 (t, 4nH, OC<u>H</u>$_2$C<u>H</u>$_2$O), 3.35 (s, 3H, OC<u>H</u>$_3$), 3.24 (m, 2H, C<u>H</u>$_2$NH—(C=O)—NH), 3.16 (m, 2H, C<u>H</u>$_2$NH—(C=O)—OCH$_2$), 2.23 (s, 3H, C<u>H</u>$_3$, UPy), 1.59–1.35 (3m, 8H) ppm.

FT-IR (ATR): υ = 3320, 2875, 1700 (UPy), 1670 (UPy), 1620 (urea), 1580 (UPy), 1530 (UPy), 1470, 1420, 1400, 1370, 1290, 1240, 1185 (C—O stretch), 1110, 1040, 940, 840, 810, 770, 740 cm^{-1}.

Synthesis of Monohydroxytelechelic PCL

The monohydroxy-telechelic PCL of the assumed molar mass (i.e., M_n controlled by the consumed monomer to transfer agent concentrations ratio) was prepared by the CL polymerization initiated with $Sn(Oct)_2$ and 1-butanol (BuOH) as an initiator.[40] Typically, 1-butanol (23.8 µL, 0.26 mmol) and CL (3.2 mL, 30 mmol) were charged in a 50-mL Schlenk flask with a magnetic stirring bar, and a solution of $Sn(Oct)_2$ (8 µL, 0.024 mmol) in 2 mL of toluene was added using a syringe. The reactive mixture was degassed via three pump–freeze–thaw cycles and then immersed in a thermostated oil bath at 120 °C for 4 h. The resulting PCL, after deactivation of the growing species with 2 N HCl_{aq} was washed with distilled water (up to neutral pH) and lyophilized under reduced pressure (2.24 g; yield: 70%, $M_{n,GPC} = 7650$, $M_w/M_n = 1.32$).

^{1}H-NMR (CDCl$_3$): $\delta = 4.18$ (t, 2H, CH$_2$—(C=O)—OC$\underline{H}_2$ CH$_2$CH$_2$CH$_3$), 4.06 (t, 2nH, CH$_2$—(C=O)—OC$\underline{H}_2$), 3.65 (t, 2H, HO—C$\underline{H}_2$CH$_2$CH$_2$CH$_2$CH$_2$—(C=O)), 2.31 (m, 2nH, C$\underline{H}_2$—(C=O)—OCH$_2$), 1.64 (m, 4nH, CH$_2$—(C=O)—OCH$_2$C$\underline{H}_2$CH$_2$C$\underline{H}_2$CH$_2$), 1.58 (m, 4H, CH$_2$—(C=O)—OCH$_2$C$\underline{H}_2$CH$_2$CH$_3$), 1.39 (m, 2nH, CH$_2$—(C=O)—OCH$_2$CH$_2$C$\underline{H}_2$CH$_2$CH$_2$), 0.96 (t, 3H, CH$_2$—(C=O)—OCH$_2$CH$_2$CH$_2$C$\underline{H}_3$) ppm.

FT-IR (ATR): $\upsilon = 2940$, 2865, 1720 (C=O stretch), 1470, 1420, 1400, 1370, 1290, 1240, 1185 (C—O stretch), 1110, 1065, 1045, 1015, 995, 965, 940, 879, 880, 800, 785, 770, 740 cm^{-1}.

Synthesis of UPy-End Functionalized PCL (PCL-UPy)

Synthesis of UPy-PCL carried out according to the following procedure[39]: After addition of PCL (1530 mg, 0.2 mmol; $M_n = 7650$ dried 2 h under vacuum at room temperature), UPy-isocyanate (0.176 mg, 0.6 mmol) in 50 mL round bottom flask were dissolved in 30 mL chloroform and dibutyltindilaurate (10 drops DBTL as catalysis) was added. The resulting solution was stirred overnight at 60 °C and filtered to remove the urea product and precipitated in cold hexane and dried overnight under high vacuum (1.3 g; yield: 85%).

^{1}H-NMR (CDCl$_3$): $\delta = 13.13$ (s, 1H, C—N$\underline{H}$—C=N, UPy), 11.76 (s, 1H, CH$_2$NH—(C=O)—N$\underline{H}$, UPy), 10.14 (s, 1H, CH$_2$N$\underline{H}$—(C=O)—NH, UPy), 5.85 (s, 1H, C=C$\underline{H}$, UPy), 4.90 (s, 1H, CH$_2$N$\underline{H}$—(C=O)—OCH$_2$), 4.18 (t, 2H, CH$_2$—(C=O)—OC$\underline{H}_2$CH$_2$CH$_2$CH$_3$), 4.06 (t, 2nH, CH$_2$—(C=O)—OC$\underline{H}_2$), 3.24 (m, 2H, C$\underline{H}_2$NH—(C=O)—NH), 3.16 (m, 2H, C$\underline{H}_2$NH—(C=O)—OCH$_2$), 2.31 (m, 2nH, C$\underline{H}_2$—(C=O)—OCH$_2$), 2.23 (s, 3H, C$\underline{H}_3$, UPy), 1.64 (m, 4nH, CH$_2$—(C=O)—OCH$_2$C$\underline{H}_2$CH$_2$C$\underline{H}_2$CH$_2$), 1.58 (m, 4H, CH$_2$—(C=O)—OCH$_2$C$\underline{H}_2$CH$_2$CH$_3$), 1.50 (m, 8H, NH—(C=O)—NH—CH$_2$C$\underline{H}_2$C$\underline{H}_2$C$\underline{H}_2$C$\underline{H}_2$CH$_2$—NH—(C=O)—O), 1.39 (m, 2nH, CH$_2$—(C=O)—OCH$_2$CH$_2$C$\underline{H}_2$CH$_2$CH$_2$), 0.96 (t, 3H, CH$_2$—(C=O)—OCH$_2$CH$_2$CH$_2$C$\underline{H}_3$) ppm.

FT-IR (ATR): $\upsilon = 3320$ (N—H), 2940, 2865, 1720 (C=O stretch), 1700 (UPy), 1670 (UPy), 1620 (urea), 1580 (UPy), 1530 (UPy), 1470, 1420, 1400, 1370, 1290, 1240, 1185 (C—O stretch), 1110, 1065, 1045, 1015, 995, 965, 940, 879, 880, 800, 785, 770, 740 cm^{-1}.

Modification of MMT-(CH$_2$CH$_2$OH)$_2$ with UPy-Isocyanate (UPy-MMT)

Quaternary ammonium salt modified natural MMT(CH$_2$CH$_2$OH)$_2$ (1 g, 1.22 mmol, OH content) was added in round bottom flask and dried under vacuum at 90 °C for 30 min and then UPy-isocyanate (0.64 mg, 2.44 mmol) and chloroform (50 mL) were added.[41] This mixture was flushed with nitrogen for 30 min in chloroform (30 mL), and it was heated to 60 °C for 18 h with continuous stirring. The organomodified clays were then collected by filtration with a cold silica filter, washed with chloroform to remove any unreacted UPy-isocyanate, and finally dried in vacuum (1.28 g; yield: 78%).

FT-IR (ATR): $\upsilon = 3640$ (O—H), 2940 (C—H), 2865 (C—H), 1700 (UPy), 1670 (UPy), 1620 (urea), 1580 (UPy), 1530 (UPy), 1325, 1250, 1240, 1185 (C—O stretch), 1020 (Si—O) cm^{-1}.

Preparation of Polymer/MMT Nanocomposites by UPy-Based Hydrogen-Bonding System

The organomodified clay (MMT-UPy, 3%, 5%, 10%, and 20% of the polymer by weight) and polymer (0.07 mmol of PEG-UPy or PCL-UPy) and chloroform (20 mL as solvent) were mixed in a round bottom flask. The reaction mixture was degassed by three freeze–pump–thaw cycles and left in vacuum. The mixture was placed in a thermostated oil bath at 50 °C for 16 h. At the end of hydrogen bonding reaction, the mixture was precipitated into diethylether, filtered, dried, and weighed.

Characterization

Molecular weights were determined by gel permeation chromatography (GPC) using an instrument consisting of a Viscotek GPCmax Autosampler, a pump, three ViscoGEL GPC columns (G2000H$_{HR}$, G3000H$_{HR}$ and G4000H$_{HR}$), and a Viscotek differential refractive index (RI) detector with a THF flow rate of 1.0 mL/min at 30 °C. The RI detector was calibrated with polystyrene standards having narrow molecular weight distribution. Data were analyzed using Viscotek OmniSEC Omni-01 software. The powder X-ray diffraction (XRD) measurements were performed on a PANalytical X'Pert PRO X-ray diffractometer equipped with graphite-monochromatized CuK_α radiation ($\lambda = 1.15$ Å). Differential scanning calorimetry (DSC) was performed on a Perkin-Elmer Diamond DSC with a heating rate of 20 °C/min under nitrogen flow (20 mL/min). TGA was performed on a Perkin-Elmer Diamond TA/TGA with a heating rate of 10 °C /min under nitrogen flow (200 mL/min). Transmission electron microscopy (TEM) imaging of the samples was carried out on a FEI Tecnai^{TM} G^2 F30 instrument operating at an acceleration voltage of 200 kV. Ultrathin TEM specimens (about 100 nm) were prepared by using a cryo-ultramicrotome (EMUC$_6$ + EMFC$_6$, Leica) equipped with a diamond knife. The ultrathin samples were placed on holey carbon-coated grids for TEM analyses.
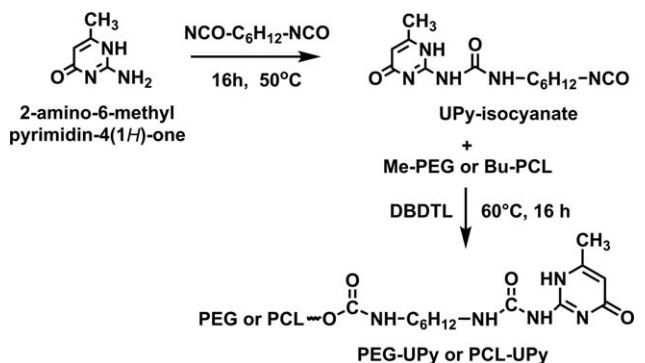
SCHEME 1 Synthesis of UPy-PEG and UPy-PCL monotelechelics.

RESULTS AND DISCUSSION

Synthesis and Characterization of UPy-End Functionalized Polymers

After discovery of UPy-based supramolecular polymers, an isocyanate-functionalized UPy (UPy-NCO) synthon was developed for end-functionalization of any hydroxyl or amine-terminated polymers, forming urethane and urea linkages.[42,43] The UPy-NCO compound was prepared by reacting 2-amino-4-hydroxyl-6-methyl pyrimidine and 1,6-hexamethylene diisocyanate. On the other hand, monohydroxytelechelic PCL was prepared via ring-opening polymerization of epsilon caprolactone initiated with $Sn(Oct)_2$ and 1-butanol. Whereas, commercially available poly(ethylene glycol) methyl ether has been used directly as received. The next step, UPy-poly(ethylene glycol) (UPy-PEG) and poly(ε-caprolactone) (UPy-PCL) have been prepared from UPy-NCO synthon with corresponding monohydroxytelechelics polymers via urethane formation at 60 °C for 16 h (Scheme 1).

The end-group transformations of monohydroxyl end functionalized polymers into UPy group were followed by ^{1}H-NMR and Fourier transform infrared (FT-IR) techniques. The ^{1}H NMR of the products showed all the characteristic signals corresponding to UPy-PEG and UPy-PCL. The transformation of —NCO group can be also seen from the FT-IR spectra, the C=O stretching peaks at 1670 and 1580 cm^{-1} were observed after the reaction, which indicates the successful attachment of pyrimidinone groups to the polymers (see "Experimental" section).

### Functionalization of Organomodified Nanoclay with UPy-Isocyanate

For the incorporation of UPy units into clay layers, UPy-NCO synthon was used to react with commercial montmorillonite clay containing two hydroxyl groups Cloisite 30B [MMT-$(CH_2CH_2OH)_2$] in chloroform (Scheme 2).

The successful incorporation of UPy groups into the clay surface was confirmed by FT-IR and XRD analyses. The FT-IR spectrum of resulting UPy-MMT showed that a characteristic isocyanate absorbance peak at 2275 cm^{-1} disappeared completely after reaction of UPy-NCO with hydroxyl groups of

MMT-$(CH_2CH_2OH)_2$ while the other peaks associated with UPy were still present. In addition, a broad peak at around 3400 cm^{-1} indicates that small amount of non-functionalized hydroxy groups on the surface of the layers was still remained. On the other hand, the XRD diffraction peak was shifted to a lower angle (from 4.89° to 4.75°) after modification, indicating an increase of the interlayer distance of the clay sheets of 0.5 nm for the UPy-MMT. The degree of UPy surface functionality was determined by TGA, which was performed to calculate the organic content of organomodified clays. The mass losses were determined as 20.3% and 42.7% MMT-$(CH_2CH_2OH)_2$ and UPy-MMT, respectively. This change indicated that the UPy-NCO synthon was successfully intercalated into the silicate galleries of the MMT clay (see Table 1).

Preparation of Polymer/MMT Nanocomposites by UPy-Based Hydrogen-Bonding System

Strong attractive interactions between the surface of an organoclay and a polymer matrix must exist in order to achieve a high degree of dispersion in organoclay nanocomposites. Among the intermolecular forces including (i) ionic interactions, (ii) ion–dipole interactions, (iii) hydrogen bonding, (iv) dipole–dipole interactions, and (v) van der Waals interactions, the hydrogen bonding is typically much stronger than Van der Waals interactions but weaker than ionic interactions. The strength of a hydrogen bonding motif is determined by the number of individual hydrogen bonds involved. To achieve a good macromolecular association, a higher hydrogen bonding association constant K is needed. One of the best-known examples is the multiple hydrogen bonding motif based on UPy group that dimerizes with a strong self-association constant ($K_{dim} > 10^7$ M^{-1} in chloroform) using a self-complementary DDAA (donor–donor–acceptor–acceptor). Another key feature of UPy motif over other hydrogen bonding groups is related to its easy chemistry; it can be attached to many different building blocks. By choosing suitable building blocks, many thermally reversible polymers have been prepared.
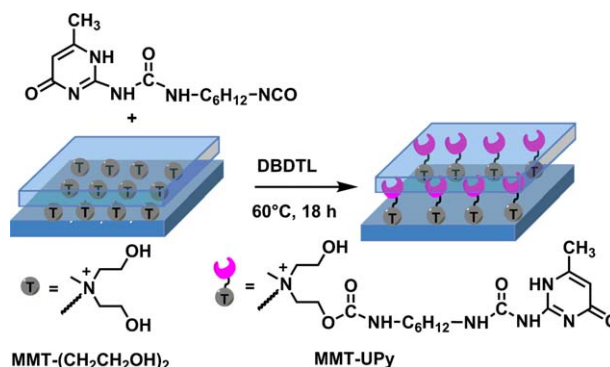
SCHEME 2 Functionalization of MMT-$(CH_2CH_2OH)_2$ with UPy-isocyanate. [Color figure can be viewed in the online issue, which is available at wileyonlinelibrary.com.]

TABLE 1 Physical Properties of PEG/MMT and PCL/MMT Nanocomposites and Their Components for Comparison

Entry	d_{001}[a] (nm)	T_m[b] (°C)	Weight Loss Temperature[c] (°C) 10%	50%	Char Yield[c] (%)
MMT	1.82	–	570	–	79.7
MMT-UPy	1.87	–	256	–	57.3
PEG-UPy	–	54.7	328	389	–
PCL-UPy	–	57.5	338	388	–
PEG/MMT-3	n.d.[d]	54.9	333	394	2.0
PEG/MMT-5	n.d.	55.3	341	397	4.8
PEG/MMT-10	3.69	55.5	344	400	9.6
PEG/MMT-20	3.74	55.6	353	404	18.7
PCL/MMT-3	n.d.	58.1	355	390	2.7
PCL/MMT-5	n.d.	58.8	360	393	4.2
PCL/MMT-10	3.91	59.4	366	399	9.4
PCL/MMT-20	3.96	59.9	371	404	18.2

[a] Basal spacing (d_{001}) is calculated by XRD analysis.
[b] Determined by DSC and analyses under a nitrogen flow at a heating rate of 10 °C/min.
[c] Determined by TGA analysis under a nitrogen flow at a heating rate of 10 °C/min.
[d] Probably complete exfoliated nanocomposites.

In order to take advantage of multiple hydrogen-bonding interactions based UPy chemistry, a series of nanocomposites were prepared by solution blending of the MMT-UPy (MMT-UPy, 3%, 5%, 10%, and 20% of the polymer by weight) with either PEG-UPy or PCL-UPy in chloroform (Scheme 3).

The infrared absorption spectra of PEG/MMT-20, PCL/MMT-20 nanocomposites, and their components were recorded in the region from 600 to 4000 cm^{-1}, as shown in Supporting Information Figures S1 and S2. The FT-IR spectra of the two samples clearly exhibited the characteristic absorptions bands that were attributable to PEG-UPy, PCL-UPy, and MMT-UPy. The characteristic bands of PEG-UPy (3320 (N—H), 2875 (C—H), 1700 (UPy), 1670 (UPy), 1620 (urea), 1580 (UPy), 1530 (UPy), 1185 (C—O stretch)) and PCL-UPy (3320 (N—H), 2940 (C—H), 2865 (C—H), 1720 (C=O stretch), 1700 (UPy), 1670 (UPy), 1620 (urea), 1580 (UPy), 1530 (UPy), 1185 (C—O stretch)) samples appeared in these spectra with insignificant shifting. The new band that appeared in the region of 1040 cm^{-1} was attributed to Si—O stretching band of MMT-UPy and was indicating the existence of nanoclays in the polymer matrices where the polymer chain was inserted between the layers of the MMT by multiple hydrogen bonding interactions.

The Morphology of PEG/MMT and PCL/MMT Nanocomposites

The XRD, DSC, and TGA results of PEG/MMT and PCL/MMT nanocomposites with various nanoclay loadings were collected in Table 1. After the nanocomposites formation, the XRD peak of MMT-UPy (4.75°) disappeared in the diffraction patterns of the nanocomposites with 3% and 5% loadings, which indicated the formation of exfoliated structures. In addition, the PEG/MMT-10, PEG/MMT-20, PCL/MMT-10, and

PCL/MMT-20 samples exhibited small and broad peaks that might be resulting from partially exfoliated or intercalated structures with d-spacings of 3.69, 3.74, 3.91, and 3.96 nm, respectively. The amount of clay in the polymer matrix is an important parameter for the complete exfoliation. By increasing clay contents, the agglomerated structures became denser in the polymer matrix and it could be more difficult to overcome the intensive ionic attraction between the neighboring platelets.[8]

The XRD analysis is a useful screening tool for determining if any sort of nanocomposites, but its reliability is limited due to the clay dilution, preferred orientation, mixed layering, and other peak broadening factors. It can be used with direct imaging techniques such as atomic force microscopy (AFM), scanning electron microscopy (SEM), or TEM to
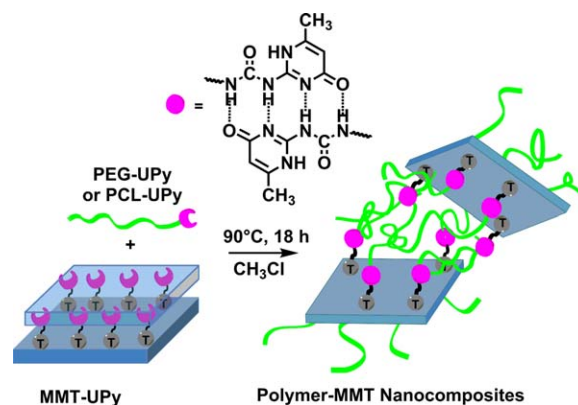
SCHEME 3 Preparation of PEG/MMT and PCL/MMT nanocomposites. [Color figure can be viewed in the online issue, which is available at wileyonlinelibrary.com.]
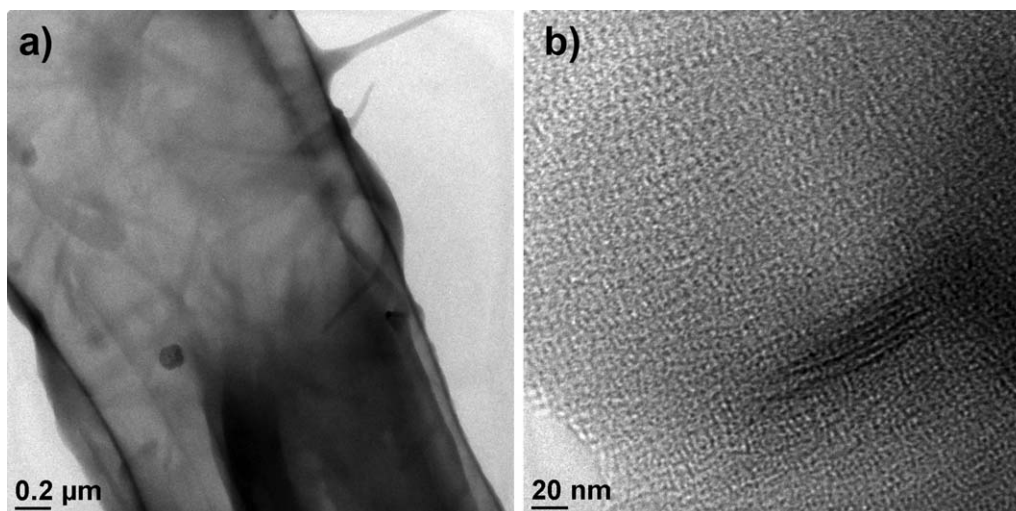
FIGURE 1 TEM micrographs of PEG/MMT-5 in low (**a**, scale bar: 200 nm) and high (**b**, scale bar: 20 nm) magnifications.

define the exact nature of the nanocomposites. TEM images of selected PEG/MMT-5 nanocomposite were provided in Figure 1 at different magnifications. The silicate layers appear as dark gray lines about 1.0 nm thick and from 50 to 100 nm in lateral dimension and the gray/white areas represent the polymer matrix.

The low magnification TEM image [Fig. 1(a)] clearly showed that most silicate layers were exfoliated and dispersed in the polymer matrix homogenously. Moreover, the intercalated silicate layers were locally stacked in some regions of polymer matrix. The low magnification image showed the general dispersion of silicate layers in the polymer matrix, whereas a high magnification image [Fig. 1(b)] clearly identified multi-layer platelets of organoclay.

The TEM images of PCL/MMT also displayed the mixed morphologies including intercalated layers with a non-uniform

separation and exfoliated single layers isolated from any stack (Fig. 2). Although it was not detected a peak in the XRD pattern for this sample, there was still intercalated structure in this sample. Combined together with XRD and TEM results, it could be concluded that partially exfoliated/intercalated structures were achieved in all nanocomposites. The coexistence of mixed morphologies implied that the van der Waals force and Coulombic force between intergalleries were still strong to hold them tightly. Therefore, some of the silicate layers could not to be separated completely. Besides, the silicate layers have high specific surface area and surface energy, which may also make them tend to aggregate together rather than to disperse homogeneously in the polymer matrix, especially at high clay loadings.[27]

Thermal Behavior
Thermal behaviors of the nanocomposites were investigated by TGA and DSC analyses. Thermal stability of the
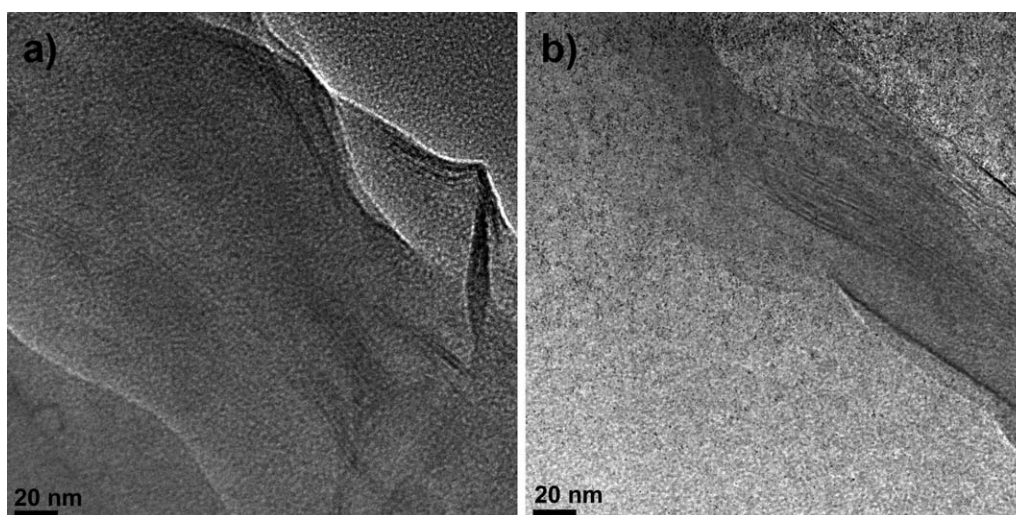

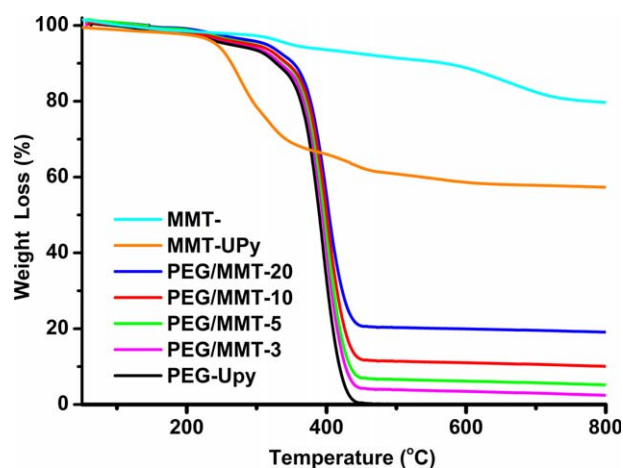**FIGURE 2** TEM micrographs of PCL/MMT-5 in high (scale bar: 20 nm) magnification.

FIGURE 3 TGA thermograms of neat PEG-UPy and resulting nanocomposites containing 3%, 5%, 10%, and 20% MMT-UPy. [Color figure can be viewed in the online issue, which is available at wileyonlinelibrary.com.]

nanocomposites was studied by TGA, heating from room temperature to 800 °C under nitrogen atmosphere to avoid thermal oxidation and to establish a more direct correlation between chemical structure and thermal degradation. The TGA results showed that all PEG/MMT samples degraded through single degradation step in the temperature range 200 °C–450 °C (Fig. 3). Thermal degradation begins at 200 °C, consistent with the degradation of UPy moieties, and accelerated at 290 °C as the PEG chains began to degrade. In order to establish the influence of the MMT content on the thermal stability of PEG, the T_{onset} (temperature at 10% weight loss) and T_{max} (temperature at 50% weight loss) were collected in Table 1. Both T_{onset} and T_{max} values of PEG/MMT samples increased almost linearly by increasing clay contents. It was clearly found that both degradation temperatures of all nanocomposites shifted significantly
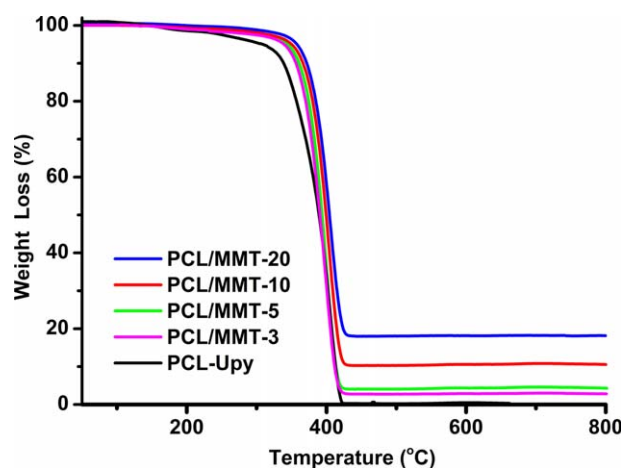

FIGURE 4 TGA thermograms of neat PCL-UPy and resulting nanocomposites containing 3%, 5%, 10%, and 20% MMT-UPy. [Color figure can be viewed in the online issue, which is available at wileyonlinelibrary.com.]
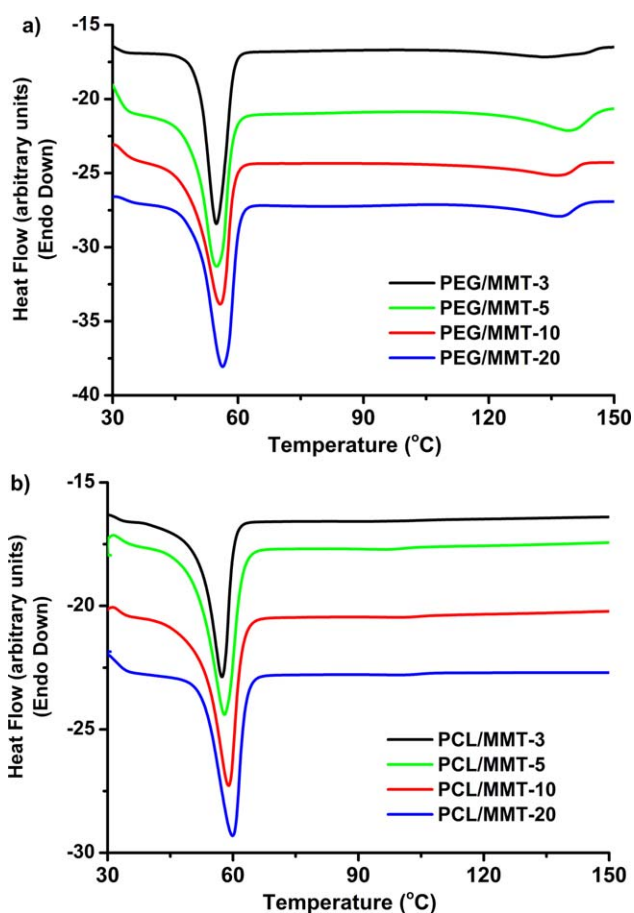

FIGURE 5 DSC traces of (**a**) neat PEG-UPy and resulting nanocomposites, (**b**) neat PCL-UPy and resulting nanocomposites. [Color figure can be viewed in the online issue, which is available at wileyonlinelibrary.com.]

toward higher temperatures compared with those of the neat PEG.

The influence of MMT on the thermal stability of PCL was also investigated for the heating rate 10 °C/min since a similar behavior was observed for all samples. From the TGA results, it was clear that T_{onset} and T_{max} temperatures of all samples moved significantly toward a higher temperature compared with those of the pristine polymer. Figure 4 confirmed that PCL/MMT nanocomposites displayed two-step mechanism of degradation containing simultaneous random chain scission and depolymerization. In the first step, pyrolysis of the ester groups which was associated with random chain scission led to release of CO_2, H_2O and hexanoic acid. For the second step, ε-caprolactone was formed as a product of an unzipping depolymerization process. The remaining mass after all organic material has been burned away gives the char yields of the nanocomposites. The char yields at 800 °C for both PEG/MMT and PCL/MMT samples were increased by increasing the clay loadings. These results demonstrated good control over clay contents in the nanocomposites. The increase in char yield also proved the reduction of the polymer's flammability and implies good thermal

stability. The final char yield of all PCL/MMT nanocomposites was improved by increasing the clay contents. The increase in char yield indicates the reduction of the polymer's flammability and implies good thermal stability.[44]

DSC analyses of neat polymers and all nanocomposites samples were carried out to determine melting temperature (T_m) values at various clay loadings (Table 1). Figure 5 showed that samples up to 20 wt % of MMT have one endothermic peak which represents melting of the crystalline phase in both PEG (54.7 °C) and PCL (57.5 °C) semicrystalline polymers. It was founded that clay loadings have no significant effect on the T_m of the nanocomposites. The nanocomposites showed a slight increase in T_m with increasing clay loadings, suggesting that the presence of silicate layers and UPy motifs led to accelerate crystalline structures in the nanocomposites formation. This observation could be attributed to the confinement of the intercalated polymer chains within the clay galleries, which prevents the segmental motions of the polymer chains. Moreover, the UPy motifs could also act as physical crosslinks and thereby increase T_m. This slight increase in crystallinity has also been observed in traditional polymer nanocomposites and reported by other groups.[45,46]

CONCLUSIONS

The organomodified clay containing self-complementary UPy motifs was successfully prepared and its structure was determined by XRD, TGA, and FT-IR analyses. A series of PEG/MMT and PCL/MMT nanocomposites have been prepared by solution blending with various clay loadings. The combined XRD and TEM results confirmed that all nanocomposites have a complex morphology with partial intercalation/exfoliation. According to TGA results, T_{onset} and T_{max} temperatures of the nanocomposites were greater than that of pristine polymers. On the other hand, T_m values of nanocomposites slightly improved by increasing clay loadings, suggesting that the addition of clay did not affect the crystallinity of the both PEG and PCL semicrystalline polymers.

ACKNOWLEDGMENTS

REFERENCES AND NOTES

1 S. S. Ray, M. Okamoto, *Prog. Polym. Sci.* **2003**, *28*, 1539–1641.

2 S. Pavlidou, C. D. Papaspyrides, *Prog. Polym. Sci.* **2008**, *33*, 1119–1198.

3 J. K. Pandey, K. R. Reddy, A. P. Kumar, R. P. Singh, *Polym. Degrad. Stabil.* **2005**, *88*, 234–250.

4 A. Okada, A. Usuki, *Macromol. Mater. Eng.* **2006**, *291*, 1449–1476.

5 E. P. Giannelis, *Adv. Mater.* **1996**, *8*, 29.

6 M. A. Tasdelen, J. Kreutzer, Y. Yagci, *Macromol. Chem. Phys.* **2010**, *211*, 279–285.

7 M. Aydin, M. A. Tasdelen, T. Uyar, Y. Yagci, *J. Polym. Sci., Part A: Polym. Chem.* **2013**, *51*, 5257–5262.

8 F. B. Barlas, D. A. Seleci, M. Ozkan, B. Demir, M. Seleci, M. Aydin, M. A. Tasdelen, H. M. Zareie, S. Timur, S. Ozcelik, Y. Yagci, *J. Mater. Chem. B* **2014**, *2*, 6412–6421.

9 Z. Yenice, M. A. Tasdelen, A. Oral, C. Guler, Y. Yagci, *J. Polym. Sci., Part A: Polym. Chem.* **2009**, *47*, 2190–2197.

10 K. D. Demir, M. A. Tasdelen, T. Uyar, A. W. Kawaguchi, A. Sudo, T. Endo, Y. Yagci, *J.Polym. Sci., Part A: Polym. Chem.* **2011**, *49*, 4213–4220.

11 C. Altinkok, T. Uyar, M. A. Tasdelen, Y. Yagci, *J. Polym. Sci., Part A: Polym. Chem.* **2011**, *49*, 3658–3663.

12 C. Dizman, S. Ates, T. Uyar, M. A. Tasdelen, L. Torun, Y. Yagci, *Macromol. Mater. Eng.* **2011**, *296*, 1101–1106.

13 A. Nese, S. Sen, M. A. Tasdelen, N. Nugay, Y. Yagci, *Macromol. Chem. Phys.* **2006**, *207*, 820–826.

14 A. Oral, M. A. Tasdelen, A. L. Demirel, Y. Yagci, *J. Polym. Sci., Part A: Polym. Chem.* **2009**, *47*, 5328–5335.

15 R. Bongiovanni, E. A. Turcato, A. Di Gianni, S. Ronchetti, *Prog. Org. Coat.* **2008**, *62*, 336–343.

16 S. Ceccia, E. A. Turcato, P. L. Maffettone, R. Bongiovanni, *Prog. Org. Coat.* **2008**, *63*, 110–115.

17 A. Di Gianni, E. Amerio, O. Monticelli, R. Bongiovanni, *Appl. Clay Sci.* **2008**, *42*, 116–124.

18 A. Di Gianni, R. Bongiovanni, L. Conzatti, S. Turri, *J. Colloid Interf. Sci.* **2009**, *336*, 455–461.

19 G. Malucelli, R. Bongiovanni, M. Sangermano, S. Ronchetti, A. Priola, *Polymer* **2007**, *48*, 7000–7007.

20 M. A. Tasdelen, Y. Yagci, *Aust. J. Chem.* **2011**, *64*, 982–991.

21 M. Huskic, E. Zagar, M. Zigon, *Eur. Polym. J.* **2012**, *48*, 1555–1560.

22 M. Huskic, M. Zigon, *Eur. Polym. J.* **2007**, *43*, 4891–4897.

23 M. Huskic, M. Zigon, *J. Appl. Polym. Sci.* **2009**, *113*, 1182–1187.

24 M. Huskic, M. Zigon, M. Ivankovic, *Appl. Clay Sci.* **2013**, *85*, 109–115.

25 M. A. Tasdelen, W. Van Camp, E. Goethals, P. Dubois, F. Du Prez, Y. Yagci, *Macromolecules* **2008**, *41*, 6035–6040.

26 A. Oral, M. A. Tasdelen, A. L. Demirel, Y. Yagci, *Polymer* **2009**, *50*, 3905–3910.

27 M. A. Tasdelen, *Eur. Polym. J.* **2011**, *47*, 937–941.

28 M. Aydin, M. A. Tasdelen, T. Uyar, S. Jockusch, N. J. Turro, Y. Yagci, *J. Polym. Sci., Part A: Polym. Chem.* **2013**, *51*, 1024–1028.

29 F. Schreiber, *Prog. Surf. Sci.* **2000**, *65*, 151–256.

30 G. M. Whitesides, J. P. Mathias, C. T. Seto, *Science* **1991**, *254*, 1312–1319.

31 S. H. M. Sontjens, R. P. Sijbesma, M. H. P. van Genderen, E. W. Meijer, *J. Am. Chem. Soc.* **2000**, *122*, 7487–7493.

32 K. E. Feldman, M. J. Kade, T. F. A. de Greef, E. W. Meijer, E. J. Kramer, C. J. Hawker, *Macromolecules* **2008**, *41*, 4694–4700.

33 A. T. ten Cate, H. Kooijman, A. L. Spek, R. P. Sijbesma, E. W. Meijer, *J. Am. Chem. Soc.* **2004**, *126*, 3801–3808.

34 M. Guo, L. M. Pitet, H. M. Wyss, M. Vos, P. Y. W. Dankers, E. W. Meijer, *J. Am. Chem. Soc.* **2014**, *136*, 6969–6977.

35 P. A. Delgado, M. A. Hillmyer, *RSC Adv.* **2014**, *4*, 13266–13273.

36 N. E. Botterhuis, D. J. M. van Beek, G. M. L. van Gemert, A. W. Bosman, R. P. Sijbesma, *J. Polym. Sci., Part A: Polym. Chem.* **2008**, *46*, 3877–3885.

37 M. H. Wrue, A. C. McUmber, M. Anthamatten, *Macromolecules* **2009**, *42*, 9255–9262.

38 M. G. McKee, C. L. Elkins, T. Park, T. E. Long, *Macromolecules* **2005**, *38*, 6015–6023.

39 B. J. B. Folmer, R. P. Sijbesma, R. M. Versteegen, J. A. J. van der Rijt, E. W. Meijer, *Adv. Mater.* **2000**, *12*, 874–878.

40 A. Kowalski, A. Duda, S. Penczek, *Macromolecules* **2000**, *33*, 689–695.

41 C. C. Neikirk, J. W. Chung, R. D. Priestley, *RSC Adv.* **2013**, *3*, 16686–16696.

42 S. Bobade, Y. Wang, J. Mays, D. Baskaran, *Macromolecules* **2014**, *47*, 5040–5050.

43 D. J. M. van Beek, A. J. H. Spiering, G. W. M. Peters, K. te Nijenhuis, R. P. Sijbesma, *Macromolecules* **2007**, *40*, 8464–8475.

44 A. Leszczyńska, J. Njuguna, K. Pielichowski, J. R. Banerjee, *Thermochim. Acta* **2007**, *453*, 75–96.

45 B. Lepoittevin, M. Devalckenaere, N. Pantoustier, M. Alexandre, D. Kubies, C. Calberg, R. Jérôme, P. Dubois, *Polymer* **2002**, *43*, 4017–4023.

46 D. Homminga, B. Goderis, I. Dolbnya, H. Reynaers, G. Groeninckx, *Polymer* **2005**, *46*, 11359–11365.